Role of isospin physics in supernova matter and neutron stars

Bharat K. Sharma and Subrata Pal

Department of Nuclear and Atomic Physics, Tata Institute of
Fundamental Research, Homi Bhabha Road, Mumbai 400005, India

We investigate the liquid-gas phase transition of hot protoneutron stars shortly after their birth following supernova explosion and the composition and structure of hyperon-rich (proto)neutron stars within a relativistic mean-field model where the nuclear symmetry energy has been constrained from the measured neutron skin thickness of finite nuclei. Light clusters are abundantly formed with increasing temperature well inside the neutrino-sphere for an uniform supernova matter. Liquid-gas phase transition is found to suppress the cluster yield within the coexistence phase as well as decrease considerably the neutron-proton asymmetry over a wide density range. We find symmetry energy has a modest effect on the boundaries and the critical temperature for the liquid-gas phase transition, and the composition depends more sensitively on the number of trapped neutrinos and temperature of the protoneutron star. The influence of hyperons in the dense interior of stars makes the overall equation of state soft. However, neutrino trapping distinctly delays the appearance of hyperons due to abundance of electrons. We also find that a softer symmetry energy further makes the onset of hyperon less favorable. The resulting structures of the (proto)neutron stars with hyperons and with liquid-gas phase transition are discussed.

I. INTRODUCTION

Recently considerable effort has been devoted to understand the isospin physics because of its paramount importance in determining the structure and dynamics of finite nuclei [1–3] and also in the astrophysical contexts such as supernova dynamics, protoneutron star evolutions and the structure and properties of neutron star [4–7]. In stable nuclei, the neutron-proton asymmetry, $\delta = (\rho_n - \rho_p)/(\rho_n + \rho_p)$, is about 0.2, where ρ_n and ρ_p are the neutron and proton number densities. In forthcoming rare-isotope accelerator experiments the magnitude of δ could be well above 0.24. In contrast, a large $\delta \approx 0.9$ is reached in the dense interior of neutron stars [4, 6, 8]. Whereas, very small asymmetry of $\delta \sim 0.1$ is attained near the crust of (proto)neutron stars at densities $\rho \sim 10^{-5}$-10^{-1} fm^{-3} [9, 10]. In order to understand the composition and structure of stars over this extreme values of density and asymmetry requires precise knowledge of the density dependence of nuclear symmetry energy $E_{\rm sym}(\rho)$.

Several theoretical studies have demonstrated [2, 3] that $E_{\rm sym}(\rho)$ represents the leading coefficient of an expansion of the total energy, $E(\rho, \delta)$, for a neutron-rich system with respect to asymmetry: $E(\rho, \delta) = E(\rho, 0) + E_{\rm sym}(\rho)\delta^2 + \mathcal{O}(\delta^4)$. The symmetric nuclear matter equation of state, $E(\rho, 0)$, has been already well constrained over a wide density range from analysis of a large body of data within non-relativistic models [11, 12] and relativistic models [1]. In contrast, though the nuclear symmetry energy at the normal nuclear matter density $\rho_0 = 0.15$ fm^{-3} is well constrained to $E_{\rm sym}(\rho_0) = 32 \pm 4$ MeV, its value and trend at lower and especially at higher densities are poorly known [1, 13]. Various theoretical calculations based on microscopic [14–16] and/or phenomenological many-body approaches [2, 3, 13, 17–19], though repro-

duce the well-constrained value of $E_{\rm sym}(\rho_0)$, their high density predictions of symmetry energy are extremely diverse. While certain models predict a monotonically increasing symmetry energy with density, other model results show that $E_{\rm sym}(\rho)$ increases initially up to about ρ_0 and decreases thereafter. These diverse predictions in the density dependence in the symmetry energy lead to large uncertainty in the incompressibility of symmetric nuclear matter which mainly stems due to insufficient knowledge about the isospin dependence of in-medium nuclear effective interactions.

Recently some progress has been achieved by consistently constraining the symmetry energy to $32(\rho/\rho_0)^{0.7} \leq E_{\rm sym}(\rho) \leq 32(\rho/\rho_0)^{1.1}$ at subsaturation densities from analysis of isospin diffusion [3, 20] and isoscaling [21] data in intermediate energy heavy ion collisions and from the study of neutron skin of several nuclei [22, 23]. Within a relativistic mean-field (RMF) model [17, 24, 25], the symmetry energy has been constrained to a small range [23] from analysis of neutron skin thickness of several nuclei across the periodic table. Further, the slope parameter and the incompressibility for the constrained $E_{\rm sym}(\rho)$ was found [23] consistent with that extracted from isospin diffusion and isoscaling data.

In an effort to pindown the precise density dependence of symmetry energy, it has been noted [13, 26] that the skin thickness of neutron-rich heavy nucleus, for example ^{208}Pb, are linearly correlated with the symmetry pressure at a density slightly below the normal nuclear matter value. Since the same pressure supports a neutron star at supranormal densities against gravitational collapse, suggests an underlying correlation between neutron skin of heavy nuclei and neutron star radii [26]. Within the RMF models, the constrained $E_{\rm sym}(\rho)$ demonstrated [23] that the neutron skin in ^{208}Pb tend to yield smaller neutron star radii. Furthermore, within the constrained range of

symmetry energy, significant sensitivity on several features of liquid-gas phase transition [27, 28] in hot asymmetric nuclear matter was found [29]. In particular, the boundary and area of the liquid-gas coexistence region, the maximal isospin asymmetry and the critical values of pressure and isospin asymmetry all of which systematically increase with increasing overall softness of $E_{\rm sym}(\rho)$.

It is thus instructive to explore the effects of symmetry energy in the RMF model, that has been limited to a narrow range from analysis of skin data, on the composition and structure of hot protoneutron and cold neutron star matter that encompasses a large density range. A newly born neutron star or protoneutron star (PNS) [5, 9, 10, 30] is formed in the aftermath of a successful supernova explosion and subsequent gravitational collapse of the core of a massive star. Due to short mean free path of neutrinos of $\lambda_\nu \sim 10$ cm (compared to PNS radii of about 10 km), the neutrinos are trapped temporarily within the neutrino-sphere of the star. The PNS are thus rich in leptons, mostly e^- and ν_e, and quite hot with central temperatures of $T = 10-50$ MeV. Thus the star matter has the interesting possibility to undergo liquid-gas phase transition close to the surface of the star [31, 32], the characteristics of which is mainly controlled by the symmetry energy at subsaturation densities. In the much longer Kelvin-Helmholtz evolution stage of about 10 sec, the neutrinos escape from the interior, and the hot and lepton-rich PNS changes into a cold and deleptonized neutron star. The loss of neutrinos enforce the electrons and protons to combine resulting in a neutron-rich neutron star matter. Consequently, the symmetry energy at supranormal densities plays an important role in determining the composition, in particular the possible presence of strange hyperons, the structure (mass and radius) and the long-term cooling of the neutron star.

In this paper we study the role of isospin on the liquid-gas phase transition in hot lepton-rich protoneutron star and the properties of (proto)neutron star within the ac-

curately calibrated parameter set FSUGold [25] in the relativistic mean-field (RMF) model. For this purpose, we restrict the model density dependence of symmetry energy $E_{\rm sym}(\rho)$ within a narrow range that reproduced the skin thickness of several nuclei [23]. At the supranormal densities the contribution of the hyperon degrees of freedom to the equation of state of the star is considered. At very low densities well below the saturation value, that is relevant to the crust, few-body correlations become important. The system can then minimize its energy via the formation of medium-modified light clusters [33, 34] which eventually dissolve into homogeneous nuclear matter at higher densities due to Pauli blocking.

The paper is organized as follows: In Sec. II we introduce the RMF model for baryons along with the medium-modified clusters. The construction of the liquid-gas phase transition in the hot protoneutron star matter is presented. In Sec. III the numerical results for the structure and composition of the star matter are discussed. Sec. IV summarizes the results.

II. FORMALISM

A. The RMF Model with clusters

We consider the relativistic mean-field (RMF) model with all the charge states of the baryon octet ($B \equiv p, n, \Lambda, \Sigma^+, \Sigma^0, \Sigma^-, \Xi^0, \Xi^-$) and their antiparticles. Light clusters ($C \equiv {}^2{\rm H}, {}^3{\rm H}, {}^3{\rm He}, {}^4{\rm He} \equiv d, t, h, \alpha$), that are treated as quasi-particles, are also included as explicit degrees of freedom. The properties of these clusters are modified by medium effects via the temperature-dependent shifts in the binding energies as treated in Ref. [33, 34]. The interaction Lagrangian density in the nonlinear RMF model [25, 34, 35] for a system of baryons, clusters and leptons for protoneutron star matter is given by

$$\mathcal{L} = \sum_{i=B,t,h} \overline{\psi}_i \left(\gamma_\mu i D_i^\mu - m_i^* \right) \psi_i + \frac{1}{2} (i D_\alpha^\mu \phi_\alpha)^* (i D_{\alpha\mu} \phi_\alpha) - \frac{1}{2} m_\alpha^{*2} \phi_\alpha^* \phi_\alpha + \frac{1}{4} (i D_d^\mu \phi_d^\nu - i D_d^\nu \phi_d^\mu)^* (i D_{d\mu} \phi_{d\nu} - i D_{d\nu} \phi_{d\mu})$$

$$- \frac{1}{2} m_d^{*2} \phi_d^{\mu*} \phi_{d\mu} + \frac{1}{2} (\partial_\mu \sigma \partial^\mu \sigma - m_\sigma^2 \sigma^2) - \frac{\kappa}{3!} (g_{\sigma N} \sigma)^3 - \frac{\lambda}{4!} (g_{\sigma N} \sigma)^4 - \frac{1}{4} \omega_{\mu\nu} \omega^{\mu\nu} + \frac{1}{2} m_\omega^2 \omega_\mu \omega^\mu + \frac{\zeta}{4!} \left(g_{\omega N}^2 \omega_\mu \omega^\mu \right)^2$$

$$- \frac{1}{4} \boldsymbol{\rho}_{\mu\nu} \cdot \boldsymbol{\rho}^{\mu\nu} + \frac{1}{2} m_\rho^2 \boldsymbol{\rho}_\mu \cdot \boldsymbol{\rho}^\mu + \Lambda_v \left(g_{\rho N}^2 \boldsymbol{\rho}_\mu \cdot \boldsymbol{\rho}^\mu \right) \left(g_{\omega N}^2 \omega_\mu \omega^\mu \right) + \sum_l \overline{\psi}_l \left(i \gamma_\mu \partial^\mu - m_l \right) \psi_l, \tag{1}$$

where ψ_i is spin-1/2 fields for the particles ($i = B, t, h$), ϕ_α is the spin-0 field for the alpha particle, and ϕ_d^μ is the spin-1 field for deuteron all of which are coupled to the σ, ω, ρ mesons. The field strength tensors for the vector mesons are $\omega_{\mu\nu} = \partial_\mu \omega_\nu - \partial_\nu \omega_\mu$ and $\boldsymbol{\rho}_{\mu\nu} = \partial_\mu \boldsymbol{\rho}_\nu - \partial_\nu \boldsymbol{\rho}_\mu$. The nonlinear σ-meson couplings (κ, λ) soften the sym-

metric nuclear matter equation of state (EOS) at around ρ_0, while its high density part is softened by the self-interactions (ζ) for the ω-meson field. The sum on l is over the non-interacting electrons and muons (e^- and μ^-) and their antiparticles in the star.

The covariant derivative

$$iD_i^\mu = i\partial^\mu - g_{\omega i}A_i\omega^\mu - g_{\rho i}|N_i - Z_i|\boldsymbol{\tau}\cdot\boldsymbol{\rho}^\mu I_{3i}, \quad (2)$$

of the particle i with mass, proton, neutron numbers (A_i, Z_i, N_i) involves interaction with the vector mesons. Of course for hyperons ($i \equiv Y$) the (A_i, Z_i, N_i) drop out in Eq. (2) and hereafter. I_{3i} is the isospin projection of the baryon and cluster charge state i. The effective mass of the ith species is

$$m_i^* = m_i - g_{\sigma i}A_i\sigma - \Delta B_i, \quad (3)$$

where the vacuum rest mass of the clusters $i = d, t, h, \alpha$ is given by $m_i = Z_i m_p + N_i m_n - B_i^0$. For the vacuum binding energy B_i^0 of the clusters we adopt the experimentally measured values. Note the clusters which are predominant at densities $\rho \sim (10^{-5}-10^{-1})\rho_0$ are treated as structureless point particles. The scalar isovector $a_0(980)$ (the δ meson) that splits the effective masses of the baryons has not been included in the present study as its effects on the star properties were found to be minimal [8, 36]. The medium dependent shift of the binding energy ΔB_i that appears only for the clusters are adopted from Ref. [34]. For nuclei embedded in nuclear matter, the shift has been calculated by solving the in-medium Schrödinger equation which leads to the ground state energy [34]

$$B_{A,Z} = B_{A,Z}^0 + \frac{K^2}{2Am} + \Delta B_{A,Z}^{SE} + \Delta B_{A,Z}^{Pau} + \Delta B_{A,Z}^{Cou}. \quad (4)$$

The shift due to self-energy, $\Delta B_{A,Z}^{SE}$, is already contained in the effective particle mass in the RMF model. The Coulomb shift, $\Delta B_{A,Z}^{Cou}$, that can be evaluated within the Wigner-Seitz approximation gives a small value for the light clusters and thus neglected. The dominant contribution emerge from the Pauli shift, $\Delta B_{A,Z}^{Pau}$, that has been evaluated in the perturbation theory with Jastrow and Gaussian approaches for d and (t, h, α), respectively. We adopt the empirical form for Ref. [34]

$$\Delta B_i(\rho_p^{\text{tot}}, \rho_n^{\text{tot}}, T) = -\tilde{\rho}_i\Big[1 + \frac{\tilde{\rho}_i}{2\tilde{\rho}_i^0(T)}\Big]\delta B_i(T), \quad (5)$$

where $\tilde{\rho}_i = 2(Z_i\rho_p^{\text{tot}} + N_i\rho_n^{\text{tot}})/A_i$ and $\tilde{\rho}_i^0(T) = B_i^0/\delta B_i(T)$. The quantity $\delta B_i(T)$ can be found from Eqs. (26)-(27) in Ref. [34]. With increasing temperature and/or density a cluster will dissolve when its total binding energy $B_i = B_i^0 + \Delta B_i$ vanishes. In the above expression the total densities for neutrons, $\rho_n^{\text{tot}} = \sum_{i=B,C} N_i\rho_i$, and protons, $\rho_p^{\text{tot}} = \sum_{i=B,C} Z_i\rho_i$ are contributions from baryons (B) and clusters (C).

The composition of the star is determined by the requirements of charge neutrality and β-equilibrium conditions $B_1 \to B_2 + l + \overline{\nu}_l$, $B_2 + l \to B_1 + \nu_l$, where B_1 and B_2 are the baryons and l is a lepton (e^- or μ^-) or their respective antiparticles at finite temperature. With clusters (A, Z), these weak processes correspond to $(A, Z) \to (A, Z+1)+l+\overline{\nu}_l$ and $(A, Z)+l \to (A, Z-1)+\nu_l$.

The chemical potential of a species i with baryon number B_i, charge Q_i, and lepton number L_i in chemical equilibrium is in general

$$\mu_i = B_i\mu_B + Q_i\mu_Q + L_i\mu_L. \quad (6)$$

The three independent chemical potentials μ_B, μ_Q and μ_L can be determined from total baryon number, charge, and lepton number conservations leading to

$$\begin{aligned}
\mu_{A,Z} &= A\mu_B + Z\mu_Q, \\
\mu_{e^-} &= -\mu_{e^+} = -\mu_Q + \mu_L, \\
\mu_{\nu_l} &= -\mu_{\overline{\nu}_l} = \mu_L; \quad (l = e^-, \mu^-).
\end{aligned} \quad (7)$$

For a deleptonized neutron star, the (anti)neutrinos escape freely so that $\mu_L = 0$. The remaining chemical potentials, μ_B and μ_Q, can be obtained from conservations of total baryon and charge densities

$$\begin{aligned}
\rho &= \sum_{i=B,C} A_i\rho_i = \rho_n^{\text{tot}} + \rho_p^{\text{tot}}, \\
\rho_Q &= \sum_{i=B,C} Q_i\rho_i + \sum_{l=e,\mu} Q_l\rho_l = 0.
\end{aligned} \quad (8)$$

When neutrinos are trapped, the matter (inside the neutrino-sphere) on a dynamical time scale is characterized by a fixed lepton fraction (number of leptons per baryon), $Y_{Ll} = Y_L + Y_{\nu_l}$, for each flavor $l = e, \mu$. In fact, muons are absent in a PNS that leads to $Y_{L\mu} = 0$ and $\mu_{\nu_l} \equiv \mu_{\nu_e}$ in Eq. (7). Consequently, the composition of a hot PNS is characterized by a constant value of $Y_{Le} = Y_e + Y_{\nu_e}$, which in the late stage reaches a value of $Y_{Le} \simeq 0.4$.

The number density for a fermionic species $i = B, t, h, l$ at temperature $T \neq 0$

$$\rho_i = \frac{2J_i + 1}{(2\pi)^3} \int d^3k \left[f_i^+(k) - f_i^-(k)\right], \quad (9)$$

where J_i is the spin of the ith species and the distribution function for particles and antiparticles (referred to as $\pm$ sign) is as usual [27, 28]

$$f_i^\pm(k) = \left[\exp\left\{(E_i^*(k) \mp \nu_i)/T\right\} + 1\right]^{-1}. \quad (10)$$

The density of the bosonic species $i = d, \alpha$ is obtained from [34]

$$\rho_i = \frac{2J_i + 1}{(2\pi)^3} \int d^3k \, g_i(k) + \tilde{\rho}_i, \quad (11)$$

where $\tilde{\rho}_i$ stems from the condensed bosons in the ground state. The Bose-Einstein distribution follows as

$$g_i(k) = \left[\exp\left\{(E_i^*(k) - \nu_i)/T\right\} - 1\right]^{-1}. \quad (12)$$

For interacting baryons and clusters, the effective energy and chemical potentials are respectively $E_i^* = \sqrt{k^2 + m_i^{*2}}$ and $\nu_i = \mu_{A,Z} - g_{\omega i}A_i\omega_0 - g_{\rho i}(N_i - Z_i)\rho_{03}I_{3i}$,

where ω_0 and ρ_{03} are the timelike and isospin three component of the vector ω-meson and vector-isovector ρ-meson. For field-free lepton, these quantities reduce to $E_l^* \equiv E_l = \sqrt{k^2 + m_l^2}$ and $\nu_l = \mu_l$. The field equations for the mesons ($m = \sigma, \omega, \rho$) are derived in the usual way [27] for the Lagrangian of Eq. (1). Herein the contribution from the cluster densities to the source terms in the meson fields are consistently incorporated by noting that in the present Lagrangian the couplings g_{mi} of the meson fields to the baryons and clusters ($i = B, d, t, h, \alpha$) are constant (density independent) unlike that in Ref. [34].

At finite temperature and baryon density, the energy density and pressure corresponding to the Lagrangian of Eq. (1) can be obtained from the thermodynamical potential Ω [27] as

$$
\begin{aligned}
\mathcal{E} = \ & \frac{m_\sigma^2 \sigma^2}{2} + \frac{\kappa}{3!} (g_{\sigma N}\sigma)^3 + \frac{\lambda}{4!} (g_{\sigma N}\sigma)^4 + \frac{m_\omega^2 \omega_0^2}{2} \\
& + \frac{\zeta}{8} (g_{\omega N}\omega_0)^4 + \frac{m_\rho^2 \rho_{03}^2}{2} + 3\Lambda_v (g_{\omega N}\omega_0)^2 (g_{\rho N}\rho_{03})^2 \\
& + \sum_{i=B,t,h,l} \frac{2J_i + 1}{(2\pi)^3} \int d^3k \, E_i^*(k) \left[f_i^+(k) + f_i^-(k) \right] \\
& + \sum_{i=d,\alpha} \left[\frac{2J_i + 1}{(2\pi)^3} \int d^3k \, E_i^*(k) g_i(k) + m_i^* \tilde{\rho}_i \right], \quad (13)
\end{aligned}
$$

$$
\begin{aligned}
P = \ & -\frac{m_\sigma^2 \sigma^2}{2} - \frac{\kappa}{3!} (g_{\sigma N}\sigma)^3 - \frac{\lambda}{4!} (g_{\sigma N}\sigma)^4 + \frac{m_\omega^2 \omega_0^2}{2} \\
& + \frac{\zeta}{24} (g_{\omega N}\omega_0)^4 + \frac{m_\rho^2 \rho_{03}^2}{2} + \Lambda_v (g_{\omega N}\omega_0)^2 (g_{\rho N}\rho_{03})^2 \\
& + \sum_{i=B,t,h,l} \frac{2J_i + 1}{3(2\pi)^3} \int d^3k \, \frac{k^2}{E_i^*(k)} \left[f_i^+(k) + f_i^-(k) \right] \\
& + \sum_{i=d,\alpha} \frac{2J_i + 1}{3(2\pi)^3} \int d^3k \, \frac{k^2}{E_i^*(k)} g_i(k). \quad (14)
\end{aligned}
$$

B. Liquid-gas phase transition in PNS matter

The RMF model is applied to study the liquid-phase (LGP) transition in hot protoneutron star matter. Such a coexistence phase may occur at subsaturation densities where the star is composed of nucleons (N), clusters (C) and leptons only. A single-phase system at temperature T and density ρ is stable against LGP separation if its free energy density $\mathcal{F}$ is lower than the coexistence liquid (L) and gas (G) phase:

$$
\mathcal{F}(T, \rho, \rho_3) < (1 - \chi)\mathcal{F}^L(T, \rho^L, \rho_3^L) + \chi \mathcal{F}^G(T, \rho^G, \rho_3^G). \quad (15)
$$

The total baryon density, $\rho = \rho_p^{\text{tot}} + \rho_n^{\text{tot}}$, and the isospin density, $\rho_3 = \rho_p^{\text{tot}} - \rho_n^{\text{tot}} = -\rho\delta$, for a N-C-e-ν_e system satisfy

$$
\begin{aligned}
\rho &= (1 - \chi)\rho^L + \chi\rho^G \\
\rho_3 &= (1 - \chi)\rho_3^L + \chi\rho_3^G, \quad (16)
\end{aligned}
$$

where $\chi = V^G/V$ being the fraction of the total volume occupied by the gas phase. The stability condition, Eq. (15), implies the inequalities [27] $\partial^2 \mathcal{F}/\partial\rho^2 > 0$ and $(\partial^2 \mathcal{F}/\partial\rho^2)(\partial^2 \mathcal{F}/\partial\rho_3^2) > (\partial^2 \mathcal{F}/\partial\rho_3\partial\rho)^2$. These inequalities are equivalent to

$$
\rho \left(\frac{\partial P}{\partial \rho} \right)_{T,\delta} = \rho^2 \left(\frac{\partial^2 \mathcal{F}}{\partial\rho^2} \right)_{T,\delta} > 0, \quad (17)
$$

$$
\left(\frac{\partial \mu_p}{\partial \delta} \right)_{T,P} < 0 \quad \text{or} \quad \left(\frac{\partial \mu_n}{\partial \delta} \right)_{T,P} > 0. \quad (18)
$$

The first inequality indicates mechanical stability which means a system at positive isothermal compressibility remains stable at all densities. The second inequality corresponds to chemical stability which suggests that energy is required to alter the concentration in a stable system while maintaining temperature and pressure fixed. When one of these conditions get violated, a two-phase system is energetically favorable. The coexistence liquid-gas phase is governed by the Gibbs criteria for equal pressures and chemical potentials in the two phases with different densities but at the same temperature:

$$
\begin{aligned}
P(T, \rho^L) &= P(T, \rho^G), \quad (19) \\
\mu_i(T, \rho^L) &= \mu_i(T, \rho^G), \quad (20)
\end{aligned}
$$

where the chemical equilibrium condition refers to all the species ($i = n, p, d, t, h, \alpha, e, \nu_e$) in the system. Since we are dealing with free leptons, it is evident from Eq. (20) that the lepton density in the liquid and gas phases are identical and thus forms a common background in the baryonic matter. Else for interacting leptons, $\rho_l^L \neq \rho_l^G$, and thus the lepton number conservation would result in an additional condition similar to those of Eq. (16).

C. Symmetry energy and model parameters

The original FSUGold [25], with an isovector coupling $\Lambda_v = 0.03$, produces a soft symmetric nuclear EOS with an incompressibility $K_0 = 230$ MeV. In addition to the ground state properties of several nuclei, this model reproduces the strengths of the giant monopole resonance in ^{90}Zr and ^{208}Pb. The nucleonic matter symmetry energy for this Lagrangian at temperature $T = 0$ is given by

$$
E_{\text{sym}}(\rho) = \frac{k_{FN}^2}{6E_{FN}^*} + \frac{g_{\rho N}^2}{12\pi^2} \frac{k_{FN}^3}{m_\rho^{*2}}, \quad (21)
$$

where $E_{FN}^* = \sqrt{k_{FN}^2 + m_N^{*2}}$, and the Fermi momentum and effective mass for nucleons are k_{FN} and $m_N^* = m_N - g_{\sigma N}\sigma$, respectively. The effective ρ-meson mass is $m_\rho^{*2} = m_\rho^2 + 2g_{\rho N}^2(\Lambda_v g_{\omega N}^2 \omega_0^2)$. In asymmetric nuclear matter, the density dependence of symmetry energy has been studied [23, 26] by simultaneously varying Λ_v and $g_{\rho N}$ so that for all combinations of (Λ_v, $g_{\rho N}$) the symmetry energy is fixed at $E_{\text{sym}}(\overline{\rho}, T = 0) = 26$ MeV at

an average density $\overline{\rho}$ corresponding to $k_{FN} = 1.15$ fm^{-1}. Note the symmetry energy even at the saturation density has not been accurately constrained experimentally and only an average E_{sym} at ρ_0 is constrained by the binding energy of nuclei. Thus by following the above prescription [26] one ensures accurate binding energies and proton densities of heavy nuclei such as ^{208}Pb. In fact, only those Λ_v values were selected that reproduced the two measured observables mentioned above. For the present study we adopt $\Lambda_v = 0.0 - 0.03$ since the corresponding $E_{\text{sym}}(\rho, T = 0)$ and their slopes and curvatures are in reasonable agreement with that extracted from neutron skin thickness of several nuclei as well as the isoscaling and isospin diffusion data [23]. It may be noted that with increasing Λ_v the density dependence of symmetry energy becomes *overall* softer, i.e., softer at supranormal densities and stiffer at $\rho \lesssim \rho_0$. Within this limited Λ_v range, considerable effect on the features of liquid-gas phase transition was also observed in hot asymmetric nuclear matter [29].

The hyperon-meson coupling constants, $g_{\sigma Y}$ and $g_{\omega Y}$, are strongly correlated by the potential depth of the hyperon Y in saturated nuclear matter [8] as

$$U_Y^{(N)} = g_{\omega Y}\omega_0 - g_{\sigma Y}\sigma. \qquad (22)$$

We use SU(6) symmetry for the vector coupling constants

$$\frac{1}{3}g_{\omega N} = \frac{1}{2}g_{\omega \Lambda} = \frac{1}{2}g_{\omega \Sigma} = g_{\omega \Xi} \ ;$$

$$g_{\rho N} = \frac{1}{2}g_{\rho \Sigma} = g_{\rho \Xi}; \quad g_{\rho \Lambda} = 0 \ . \qquad (23)$$

The $g_{\sigma Y}$ couplings are adjusted to reproduce the estimated hypernuclear potential depth $U_Y^{(N)}$ at ρ_0. From detailed studies of ΛN interaction, an attractive potential depth of $U_\Lambda^{(N)} = -30$ MeV has been estimated [37] so that the observed bound Λ hypernuclear states are reproduced. Several Ξ hypernuclear states [38] and free Ξs produced in reactions [39, 40] suggest an attractive potential of $U_\Xi^{(N)} = -18$ MeV. Though the Λ and Ξ potential depths have been well studied, however, data on Σ hypernuclei are scarce and ambiguous due to strong $\Sigma N \to \Lambda N$ decay. While previous studies of hyperon stars have used an attractive Σ potential (with $U_\Sigma^{(N)} = U_\Lambda^{(N)} = -30$ MeV) that are based on the observed bound $^4_\Sigma$He hypernucleus, recent analysis [41, 42] of Σ^- atomic data point to a sizable repulsive nuclear Σ potential of depth $U_\Sigma^{(N)} = +30$ MeV. For the present study we adopt this repulsive depth of the Σ potential. This ambiguity will modify considerably the hypernuclear composition in the star, which however, has smaller effects on the bulk properties of β-equilibrated star matter.

III.   RESULTS AND DISCUSSIONS

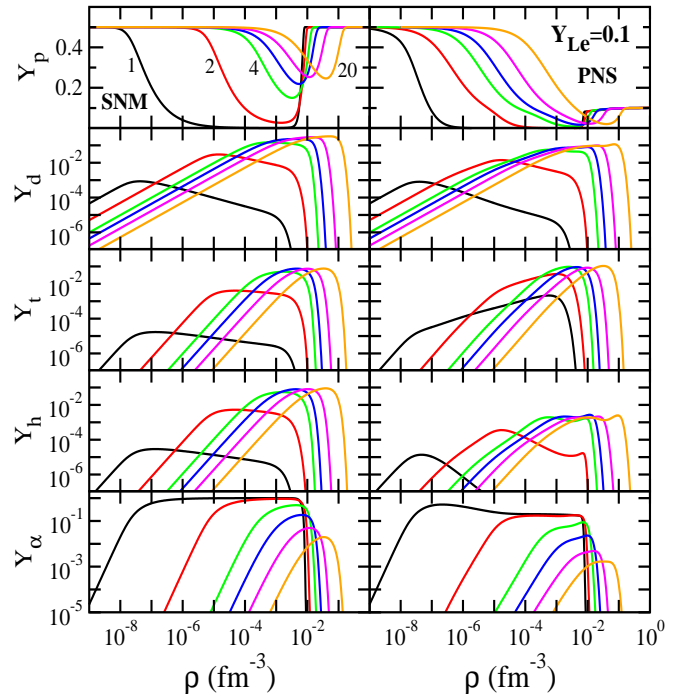We begin this section by presenting in Fig. 1 the fractions, $Y_i = A_i \rho_i / \rho$, of free protons and clusters

FIG. 1: (Color online) Density dependence of particle fractions Y_i at temperatures $T = 1, 2, 4, 6, 10, 20$ MeV in symmetric nuclear matter (SNM) and in protoneutron star (PNS) matter at a fixed lepton fraction of $Y_{Le} = 0.1$ in the FSUGold model with coupling $\Lambda_v = 0.03$.

$i = p, d, t, h, \alpha$ at various temperatures for symmetric nuclear matter (SNM: left panels) and neutrino-trapped protoneutron star (PNS: right panels) matter in the FSUGold relativistic mean-field model for the isovector coupling $\Lambda_v = 0.03$. The overall trend exhibited by symmetric matter is quite similar to that for neutron-rich protoneutron star matter. At very low densities $\rho \lesssim 10^{-7}$ where the meson fields and the baryon chemical potentials drop rapidly the PNS behaves as SNM with $Y_p = 0.5$ (see also Fig. 3). With the formation of the clusters, the threshold density of which is quite sensitive to the system temperature, the free proton fraction decreases rapidly. At a given temperature, the two-nucleon correlation results in the formation of deuteron first, followed by three-particle h, t and finally the α particle. At $T < 7$ MeV, the strongly bound alpha is seen to be the most abundant particle over a wide density range as many-body correlations gain prominence with density. Moreover, with increasing temperature, the α fraction decreases while other cluster abundances increase; the peak positions gradually shifting to higher densities. Consequently with increasing T, the minimum of Y_p increases and shifts to higher densities and then decreases again at $T \gtrsim 7$ MeV when deuterons dominate. This was also observed in the RMF model with density-dependent couplings [34]. Note that at a given temperature and density the (free) neutron-rich supernova matter has some-

what smaller cluster fractions compared to the symmetric nuclear matter. The clusters eventually dissolve due to Pauli blocking at higher densities $\rho \geq 10^{-2}$ fm^{-3} resulting in a homogeneous matter with $Y_p = 0.5$ for SNM (left panel) and a neutron-rich n-p-e-ν PNS matter (right panel).
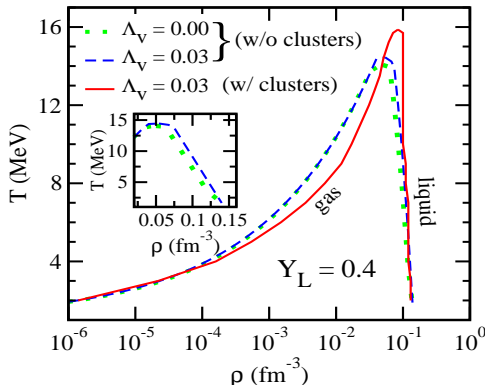

FIG. 2: (Color online) Boundary of liquid-gas phase transition in a supernova matter at a fixed lepton fraction of $Y_{Le} = 0.4$ in the FSUGold model with couplings $\Lambda_v = 0.0$ and 0.03 with and without the inclusion of clusters. The inset shows the symmetry energy effects for $\Lambda_v = 0.0$ and 0.03 at the liquid-phase boundary without clusters.

We now consider the possibility of liquid-gas phase (LGP) transition in hot and neutrino-trapped protoneutron star consisting of neutrons, protons, electrons and electron neutrino. Figure 2 shows the boundary for the existence of the coexistence phase at various temperatures in the FSUGold model for the isovector coupling $\Lambda_v = 0.0, 0.03$. The results are for electron lepton fraction $Y_{Le} \equiv Y_L = 0.4$ (and muon lepton number $Y_{L\mu} = 0$) which approximately corresponds to the value at the onset of trapping. At a nucleon density of $\rho \approx 0.08$ fm^{-3}, the critical temperature for $\Lambda_v = 0.03$ is $T_c = 14.6$ MeV which is close to that for symmetric nuclear matter [29]. Whereas a softer nuclear symmetry energy $E_{\rm sym}$ at subsaturation density ($\Lambda_v = 0$), gives a somewhat smaller T_c. In fact, the critical temperature divide the coexistence boundary into a low-density gas phase (on the left) and a high-density liquid phase (on the right) and the liquid-gas phase coexist within the boundary. Due to trapping, the net electron concentration is quite high, and the matter at the low baryon density phase is controlled by non-degenerate electrons. As a consequence, the nuclear symmetry energy corresponding to $\Lambda_v = 0$ and 0.03 has practically no effect on the gas phase boundary. On the other hand, due to dominant contribution of the degenerate nucleons in the relatively high-density liquid phase, larger effects from symmetric pressure in the stiffer $E_{\rm sym}$ for $\Lambda_v = 0.03$, shifts the liquid-phase boundary to a slightly higher density (see inset of Fig. 2). The protoneutron star matter is found to exhibit a LGP transition even at very low densities at a high temperature of $T \sim 1$ MeV.

With the inclusion of light clusters (solid line in Fig. 2), the softening of the EOS shifts the low-density coexistence phase boundary to a higher value at temperatures $T \geq 4$ MeV where clusters become abundant. On the other hand, the high-density boundary that is dominated by free nucleons is relatively unaffected. Thus the clusters effectively reduce the width of the phase coexistence region and increases the critical temperature to $T_c = 15.7$ MeV for $\Lambda_v = 0.03$ case.
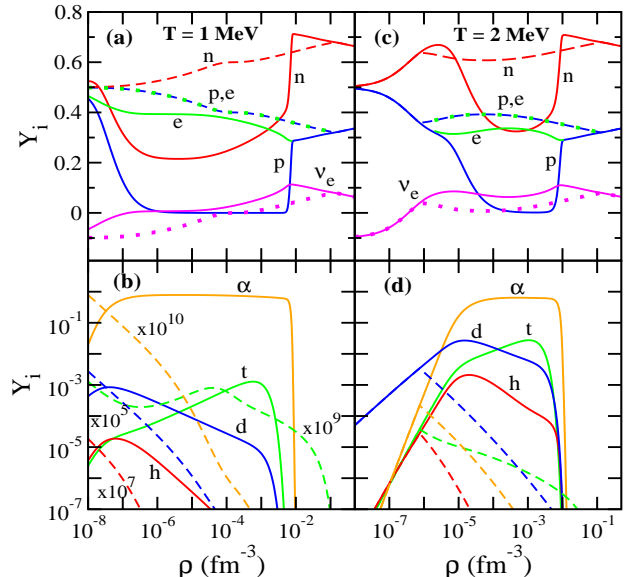

FIG. 3: (Color online) Composition of supernova matter with trapped neutrinos at a lepton fraction of $Y_{Le} = 0.4$ at a temperature of $T = 1$ and 2 MeV in the FSUGold set for $\Lambda_v = 0.03$ coupling. The results are for uniform matter (solid line) and with liquid-gas phase transition (dashed line).

In Fig. 3, the particle fractions are shown for neutrino trapped matter at an electron lepton fraction $Y_{Le} = 0.4$ at temperatures of $T = 1$ and 2 MeV for uniform matter (solid line) and in the coexistence liquid-gas phase (dashed line). One of the major effects of trapping is to enhance the net electron fraction Y_e over the entire baryon density range; the magnitude of Y_e gradually increases with Y_L. Considering first uniform matter (solid line), at $\rho \lesssim 10^{-7}$ fm^{-3}, the energy and pressure of the hot protoneutron star matter is entirely dominated by the non-degenerate electrons because of their small mass. Due to charge neutrality, the rapid rise of net electrons at this low density enforces an equally large enhancement of net number of free protons and a consequent drop in free neutron density due to baryon number conservation (see Figs. 3(a) and 3(c)). This tends to make the lepton-rich matter in this density regime highly symmetric with identical free neutron and proton fractions.

For uniform matter at higher densities, clusters dominate the particle yield (compared to free protons and neutrons especially at high T; (Figs. 3(b) and 3(d)) so that the charge neutrality is maintained primarily by the

bound protons in these clusters. Compared to $Y_{Le} = 0.1$ (Fig. 1), larger electron fraction in the present $Y_{Le} = 0.4$ case enhances the cluster production via charge neutrality. At all temperatures of interest in the supernova dynamics, we find α and deuteron to be the dominant clusters. Thus, within this density range the star matter is also highly symmetric but due to abundant symmetric cluster formation.
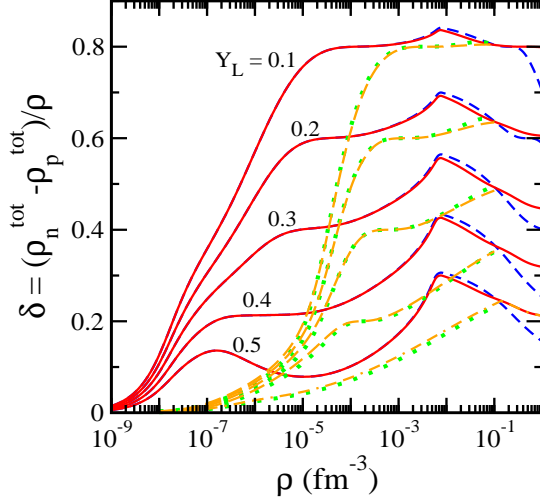

FIG. 4: (Color online) Density dependence of nuclear asymmetry δ for supernova matter with trapped neutrinos at various lepton fraction of Y_{Le} at a temperature of $T = 1$ MeV. The results are in the FSUGold set at $\Lambda_v = (0.0, 0.03)$ for uniform matter (dashed, solid line) and with liquid-gas phase transition (dotted, dash-dotted line).

With the onset of liquid-gas phase transition, it is important to note from Fig. 3 that cluster formation drops drastically (dashed lines). This stems from vanishing cluster contribution from the liquid part of the mixed phase that has a density well above the transition value where the clusters dissolve, as well as due to small cluster fraction in the gas phase that has a density smaller compared to the total ρ. Thus at small $T \lesssim 4$ MeV in the coexistence phase, Y_p is effectively enhanced and becomes identical to Y_e. This leads to the formation of n-p-e-ν matter that tends to be rather symmetric even in the coexistence phase. However, with increasing T, as the cluster fractions are large and the onset of phase transition shifts to higher ρ (see Fig. 2), considerable amount of clusters can occur in the low-density uniform phase of a hot protoneutron star. The formation of clusters and near symmetrization of the PNS matter has two major consequences. First, during the evolution of the supernova matter, the abundant light nuclei produced within the neutrino-sphere [9, 10] at densities $\rho \lesssim 10^{-5}$ fm^{-3} may be ejected outside and contribute to the nucleosynthesis of heavy elements. Second, the decrease in the pressure due to the nuclear symmetry energy overwhelms the total increase from the thermal and leptonic pressures. This makes the equation of state softer with or

without phase transition compared to the neutrino-free matter.

It may be noted from Fig. 3, that at a fixed Y_L, antineutrino $\bar{\nu}_e$ dominates over its particle counterpart at lower densities and/or in the coexistence region. Moreover, the trapping density is also shifted to a higher value in the coexistence phase. Thus, apart from neutrino transport, the exact location of the neutrino-sphere is quite sensitive to the influence of the coexistence phase in the supernova matter.
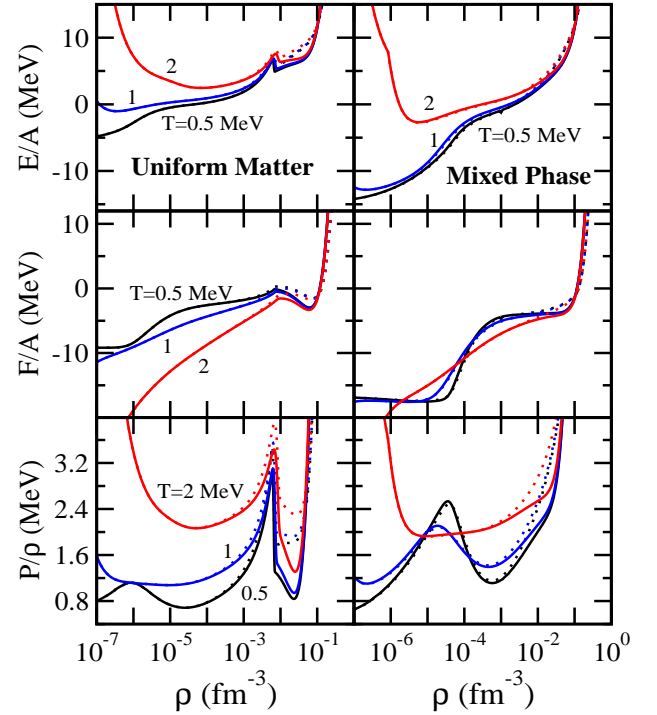

FIG. 5: (Color online) Per particle energy E/A, free energy F/A, and pressure P/ρ as a function of density for supernova matter at a lepton fraction $Y_{Le} = 0.1$ and at temperatures $T = 0.5, 1, 2$ MeV. The results are in the FSUGold set at couplings $\Lambda_v = 0.0$ (solid lines) and 0.03 (dotted lines) for uniform matter and with liquid-gas phase transition.

Figure. 4, shows the variation of neutron-proton asymmetry $\delta = (\rho_n^{\text{tot}} - \rho_p^{\text{tot}})/\rho$ with baryon density at several fixed lepton fraction Y_{Le} that correspond to the deleptonization epoch of the supernova at $T = 1$ MeV. Considering the $\Lambda_v = 0.03$ set, the dip seen in the asymmetry for uniform matter (solid lines) at $\rho \sim 10^{-2}$ fm^{-3} is due to cluster formation that increases with Y_{Le}. A further rapid drop in the asymmetry at $\rho \lesssim 10^{-7}$ fm^{-3} results from lepton dominance in the star. Thus, even in the late stage of neutrino diffusion (at small Y_L), abundant nuclei can be produced in the near-symmetric matter [31, 32]. With the onset of liquid-gas phase transition at $\rho_{\text{th}} \sim 0.1$ fm^{-3} (dash-dotted line), the asymmetry is found to decrease faster compared to the uniform matter. This stems from dominant contribution from the liquid part of the mixed phase which exhibits a dropping asym-

metry at $\rho \gtrsim \rho_{\rm th}$ (solid lines) plus a fraction from the very low-density region of the gas phase that is nearly-symmetric. Both these effects systematically favor a free energy with small δ. Thus, compared to uniform matter, the supernova matter at $T \sim 1$ MeV is found to be nearly symmetric in the coexistence phase at larger densities near the neutrino-sphere and the PNS behaves as n-p-e-ν matter. Of course at higher temperatures, the cluster contribution would be enhanced and the onset of coexistence phase is also delayed to a higher density; see Figs. 3(c)-(d). At a given ρ, this causes the PNS to be somewhat less symmetric compared to that at lower temperatures.

The sensitivity of $E_{\rm sym}$ on asymmetry δ has been also studied by considering the $\Lambda_v = 0$ set which gives an overall stiffer density dependence of symmetry energy. In this case, for uniform matter (dashed line), a larger (smaller) δ is obtained at densities smaller (larger) than the normal nuclear matter value. However, the effects of symmetry energy is negligible both at small densities that are dominated by leptons, and also in the mixed phase (dotted line).

Figure 5 depicts the equation of state (EOS) of supernova matter at $Y_{Le} = 0.1$ for uniform matter and in the coexistence phase for $\Lambda_v = 0.0$ (solid lines) and 0.03 (dotted lines) with clusters. At supranormal densities, the matter is characterized by repulsive ω-meson interaction that causes a rapid increase in the EOS. At about the normal density of $\rho_0 \approx 0.15$ fm^{-3}, the uniform matter shows a minimum for relatively small temperatures. This is a manifestation of the saturation properties of nuclear matter when thermal effects contribute modestly. A larger $E_{\rm sym}$ for the $\Lambda_v = 0.03$ at $\rho < \rho_0$ (dotted line) gives a smaller binding energy. In fact, the sensitivity of symmetry energy on the EOS persists till the contribution from free nucleons and/or clusters dominate up to a density of $\rho \sim 10^{-4}$ fm^{-3}.

In the coexistence phase, the (free) energy drops appreciably with decreasing density at small temperatures. As mentioned above, this is a consequence of the liquid part that contributes to enhance the binding of the system. The overall qualitative features found in the thermodynamic quantities with clusters are similar to those without clusters for the supernova matter (not shown). Compared to nucleons only supernova matter, the inclusion of cluster degrees of freedom reduces somewhat the total free energy. Further, the total pressure is found to be small at $\rho \sim 10^{-5}$ fm^{-3} when most of the cluster species contribute collectively. The pressure eventually becomes stiffer when only the massive alpha contributes dominantly at $\rho \sim 10^{-2}$ fm^{-3} (see inset of Fig. 7). Consequently, clusters delay the onset of the coexistence phase (situated in the soft low ρ regime of the EOS) to a higher density compared to that without clusters.

We now consider the constitution and structure of beta-equilibrated and charge neutral matter in the superdense regime. It may be noted that thermal effects contribute negligibly in this density regime where the nu-
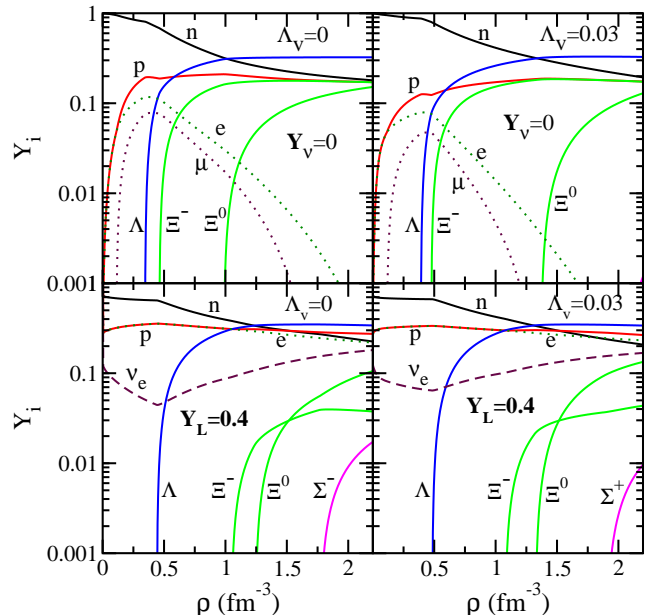

FIG. 6: (Color online) Relative concentration of beta-equilibrated matter containing nucleons and hyperons in cold lepton-poor matter ($Y_\nu = 0$) and lepton-rich matter ($Y_{Le} = 0.4$) at finite entropy per baryon $S/B = 1$ in the FSUGold set at $\Lambda_v = 0.0$ and 0.03 values for the coupling constant.

cleons become degenerate. In Fig. 6, the abundances of baryons and leptons as a function of density are shown for the FSUGold parameter sets $\Lambda_v = 0$ and 0.03 with and without the trapped neutrinos. The composition of the matter should be quite sensitive to the symmetry energy $E_{\rm sym}$ as it relates to the chemical potential via $\hat{\mu} \equiv \mu_n - \mu_p \simeq 4E_{\rm sym}\delta$ [2, 3] which in turn, determines the hyperon production threshold density by the condition $\mu_B = \mu_n - q_B(\mu_e - \mu_{\nu_e}) \geq \varepsilon_B$, where ε_B is the energy density of the baryon species B. For neutron star matter with $Y_\nu = 0$, the stiffer density dependence of symmetry energy at $\Lambda_v = 0$ causes larger enhancement of electron (and hence proton) fraction compared to $\Lambda_v = 0.03$ case. However, with the appearance of negatively charged Ξ^- hyperon which competes with leptons in maintaining charge neutrality, the lepton (e^- and μ^-) concentrations begin to fall. Consequently, the sensitivity of $E_{\rm sym}$ on the composition is diminished. The charge neutral Ξ^0 hyperon then appears, which occurs at a somewhat earlier density for the stiff symmetry energy compared to the soft $\Lambda_v = 0.03$ set.

Trapped neutrinos have a large influence on the composition of the protoneutron star as evident from Fig. 6 for $Y_{Le} = 0.4$. The appearance of hyperons is now delayed to higher densities since in the above mentioned threshold condition, the term ($\mu_e - \mu_{\nu_e}$) turns out to be positive. With the emergence of Λ hyperon, the dropping of proton and thereby the electron fraction is now compensated by the rise of ν_e abundances so that Y_{Le} is maintained constant. A softer symmetry energy ($\Lambda_v = 0.03$) is found to
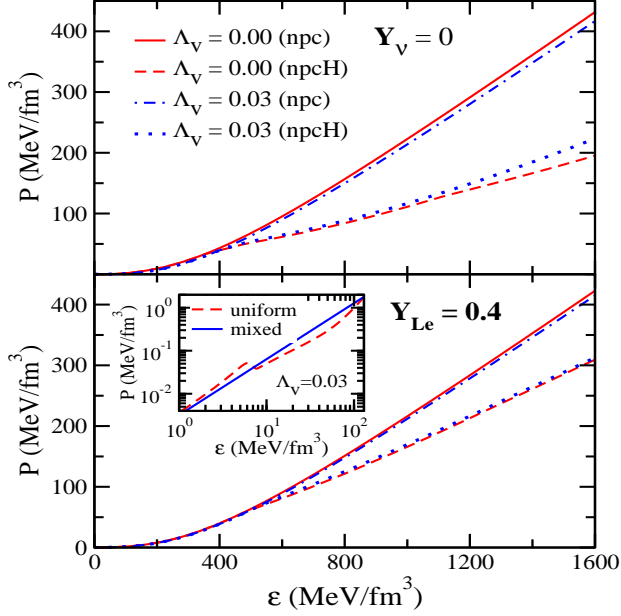
FIG. 7: (Color online) Pressure versus energy density for β-equilibrated matter with free nucleons and clusters only (npc) and with further inclusion of hyperons (npcH). The results are for cold lepton-poor matter ($Y_\nu = 0$) and lepton-rich matter ($Y_{Le} = 0.4$) at finite entropy per baryon $S/B = 1$ in the FSUGold set at $\Lambda_v = 0.0$ and 0.03 values for the coupling constant. The inset shows the equation of state of the crust for uniform matter (dashed line) and with liquid-gas mixed phase (solid line) at $\Lambda_v = 0.03$.
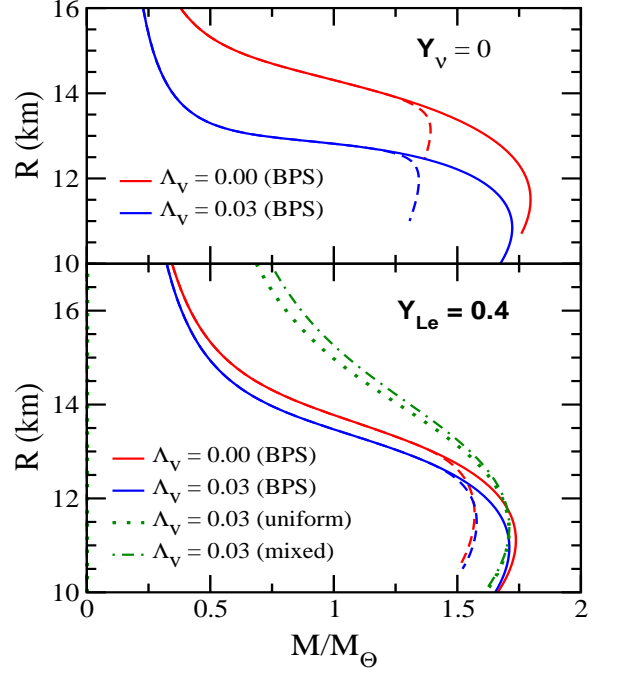

FIG. 8: (Color online) The mass-radius relation for star sequences for matter with free nucleons and clusters only (npc: solid line) and with further inclusion of hyperons (npcH: dashed line) in a cold lepton-poor matter ($Y_\nu = 0$) and lepton-rich matter ($Y_L = 0.4$) at finite entropy per baryon $S/B = 1$ in the FSUGold set at $\Lambda_v = 0.0$ and 0.03 values for the coupling constant with BPS equation of state [45] at the crust. At $Y_L = 0.4$, the results for npc star at $\Lambda_v = 0.03$ with an uniform matter (dotted line) and liquid-gas mixed phase (dash-dotted line) EOS at the surface are also shown; see text for details.

favor a significantly larger Y_{ν_e}. Incidentally, at very high densities $(\mu_e - \mu_{\nu_e})$ becomes negative. The impact of this alteration in the lepton chemical potentials is the emergence of positively charged Σ^+ before the $\Sigma^{0,-}$ hyperon. From the central densities of the maximum mass stars (see Table I), it is evident that for the repulsive potential potential of $U_\Sigma^{(N)} = +30$ MeV used here, Σ hyperons will not be present in the star matter at all. On the other hand, if we adopt an attractive interaction potential of $U_\Sigma^{(N)} = -30$ MeV, as used in previous studies, the Σ^- hyperon will appear at a density of $(2-3)\rho_0$ followed by Σ^0 and Σ^+ in the star matter. In such a situation Ξs will not appear in neutrino-trapped matter.

The equation of state (EOS), i.e. pressure P versus energy density ε is displayed in Fig. 7 for the neutrino-free matter (Y_ν) and matter with an electron lepton fraction $Y_{Le} = 0.4$ corresponding to that of Fig. 6. For nucleons-only star, trapped neutrinos makes the EOS softer as the decrease in the symmetry pressure due to enhanced proton fraction exceeds the increase in leptonic pressure. Compared to the stiff $\Lambda_v = 0$ set, a smaller symmetry energy/pressure at high density for the $\Lambda_v = 0.03$ set obviously produces a softening in the EOS. However, as a soft $E_{sym}(\rho)$ favors a large ν_e fraction [30], the softening is reduced in the lepton-rich matter. With the inclusion of hyperons, the EOS becomes softer in both lepton-rich

and lepton-poor matter. This is essentially caused by the release of the Fermi pressure of the nucleons into the hyperonic degrees of freedom, and also due to decrease of pressure exerted by the leptons as these are replaced by negatively charged hyperons [5]. However in a protoneutron star, the trapped-neutrinos inhibit the onset of hyperons (see Fig. 6) which makes the EOS with hyperons stiffer compared to the neutrino-free matter $-$ a reversal of behavior relative to the EOS for nucleons-only star matter. As evident, the comparative stiffness increases for the larger E_{sym} ($\Lambda_v = 0$) that allows relatively slightly larger hyperon population in the cold catalyzed neutron star.

The differences in the EOS should be reflected in the structure of the stars, namely their masses and radii. While most of the mass originate from the dense interior of the star, the crust has a negligible contribution of $\sim 10^{-5} M_\odot$ to the total mass. In contrast, about 40% of the radius originates from the EOS at $\rho \leq \rho_0$ and thus should be strongly influenced by the possible liquid-gas phase transition at this density regime. At first, the star sequence is calculated with the low density equation of state taken from Baym-Pethick-Sutherland

TABLE I: Maximum masses, $M_{\max}/M_\odot$, their corresponding radii, $R_{M_{\max}}$, and their central densities, ρ_c/ρ_0, of stars without ($Y_\nu = 0$) and with ($Y_{Le} = 0.2, 0.4$) trapped neutrinos; the normal nuclear matter density is $\rho_0 = 0.148$ fm^{-3}. Results are in the FSUGold mean-field model at $\Lambda_v = 0$ and 0.03.

		Without hyperons			With hyperons		
Λ_v		ρ_c/ρ_0	$M_{\max}$	$R_{M_{\max}}$	ρ_c/ρ_0	$M_{\max}$	$R_{M_{\max}}$
	$Y_\nu = 0$	7.138	1.796	11.505	4.912	1.392	13.117
0.00	$Y_{Le} = 0.2$	7.082	1.749	11.322	6.067	1.444	12.083
	$Y_{Le} = 0.4$	7.420	1.737	11.108	6.716	1.569	11.674
	$Y_\nu = 0$	7.815	1.722	10.840	5.814	1.344	11.953
0.03	$Y_{Le} = 0.2$	7.815	1.711	10.747	6.856	1.459	11.341
	$Y_{Le} = 0.4$	7.618	1.710	10.952	6.858	1.578	11.502

(BPS) of Ref. [45]; the effects of the coexistence and pure phase with clusters are discussed later. Here, the overall EOS is constructed by smoothly matching (without any discontinuity in pressure, baryon and energy densities) the BPS equation of state at $\rho < 0.001$ fm^{-3}, followed by the mixed phase EOS comprising of leptons and free nucleons only for the inner crust of the star in the RMF model, and finally with the RMF model EOS at $\rho > \rho_0$, with or without hyperons. The static star sequence obtained by solving Tolman-Oppenheimer-Volkoff equations [43] are shown in Fig. 8 for the different equations of state. Listed in Table I are the maximum masses $M_{\max}$, corresponding radii $R_{M_{\max}}$, and the central baryonic densities ρ_c. With free nucleons and leptons-only star, the trapped-neutrinos give smaller maximum mass $M_{\max}$ (compared to $Y_\nu = 0$ case) as the pressure from the stiff EOS can support larger masses against gravitational collapse. With the introduction of hyperons, the reversal of behavior observed in the EOS, i.e. trapping leads to a stiffer EOS, is manifested in larger maximum mass protoneutron stars. Note in general, the inclusion of hyperons leads to a relatively smaller mass stars due to softening of the EOS. The larger radii in stars with hyperons are a consequence of weaker gravitational attraction from smaller masses that causes the stars to be large and diffuse. For the neutrino-free stars, though $\Lambda_v = 0.03$ gives smaller masses than $\Lambda_v = 0$, the corresponding star radii are however found to be smaller in the former case.

The baryonic interactions in this model raises the maximum mass from $M_{\max} \approx 0.7 M_\odot$ for the EOS of a free gas [43] by a factor of about two for nucleons-only stars. However, the inclusion of hyperons in cold neutrino-free stars yield maximum masses that are smaller than the current observational lower limit of $1.44 M_\odot$ imposed by the larger mass of the binary pulsar PSR $1913 + 16$ [44].

The inset of Fig. 7 shows the EOS for hot matter with entropy per baryon $S/B = 1$ and $Y_{Le}=0.4$ for uniform matter (dashed line) and in the coexistence liquid-gas mixed phase (solid line). For clarity, the EOSs corresponding only to the high-density (liquid) regime of the mixed phase at volume fraction $\chi = V^G/V > 10^{-4}$ (see Eq. (15)) are shown. In fact, χ can be as low as

10^{-8} near the low-density (gas) phase boundary. Figure 8 illustrates the effect of liquid-gas phase transition at low density on the mass-radius sequence of free nucleons and clusters-only protoneutron stars for $\Lambda_v = 0.03$. Though the maximum masses are identical with $M_{\max} \approx 1.710 M_\odot$ the radii in the sequence of stars are all different. In particular, a stiff EOS obtained in the mixed phase from Gibbs construction gives consistently large radii protoneutron stars. Compared to the BPS [45] equation of state used above at $\rho < 0.001$ fm^{-3}, the RMF models in general provide much stiffer EOSs at the crust that result in stars with much larger radii.

IV. SUMMARY AND CONCLUSION

In this article, within an accurately calibrated relativistic mean field model where the nuclear symmetry energy has been constrained from measurements of neutron skin thickness of finite nuclei, the structure and properties of neutron and protoneutron stars are studied. For hot and lepton-rich protoneutron stars we examine the possible liquid-gas phase transition near the crust comprising of free nucleons and light clusters. Compared to free nucleon abundances, light clusters are found to dominate the particle yield at moderate and high temperatures in an uniform supernova matter. Further, the fraction of trapped neutrino is shown to play an important role in making the supernova matter more symmetric via enhanced production of deuteron and alpha clusters. With liquid-gas phase transition, the yields of clusters drop drastically at temperatures $T \lesssim 4$ MeV in the coexistence phase; here near symmetrization over a wide density $\rho \sim 10^{-5}-10^{-1}$ fm^{-3} is achieved by the free nucleons that are not bound in the clusters. At these low densities, symmetry energy has modest impact on the coexistence phase boundaries and on the equations of state of matter compared to thermal effects and on the number of trapped neutrinos.

The influence of symmetry energy on hyperon production in the dense interior of cold neutron stars and hot lepton-rich protoneutron stars are studied. Within the

present knowledge of the potential depth of hyperons in bulk nuclear matter, we find a repulsive potential of Σ hyperons inhibits its appearance in the star matter. Neutrino trapping delays the appearance of hyperons due to relative disposition of chemical potentials of various species. A softer symmetry energy in general result in smaller chemical potentials that delays further the onset of hyperons and thereby reduces the hyperonization of the star matter. The emergence of hyperons soften the nuclear equation of state considerably in the FSUGold model. This results in stars with very small masses especially for the cold deleptonized matter. We also find, that compared to uniform matter, a stiffer equation of state in the coexistence liquid-gas phase near the crust of hot lepton-rich matter yield stars with larger radii. The ongoing and future hypernuclear programs can provide accurate information of the potential depth of hyperons in bulk nuclear matter, which in conjunction with better mass and radius measurements of neutron stars could constrain the nuclear symmetry energy more accurately.

[1] P. Danielewicz, R. Lacey and W.G. Lynch, Science **298**, 1592 (2002).
[2] V. Baran, M. Colonna, V. Greco and M. Di Toro, Phys. Rep. **410**, 335 (2005).
[3] B.-A. Li, L.-W. Chen and C.M. Ko, Phys. Rep. **464**, 113 (2008).
[4] N.K. Glendenning, Astrophys. J. **293**, 470 (1985); Phys. Rev. D **46**, 1274 (1992).
[5] M. Prakash, I. Bombaci, M. Prakash, P.J. Ellis, J.M. Lattimer, and R. Knorren, Phys. Rep. **280**, 1 (1997).
[6] A. Steiner, M. Prakash, J.M. Lattimer and P.J. Ellis Phys. Rep. **411**, 325 (2005).
[7] J.M. Lattimer and M. Prakash, Science **304**, 536 (2004); Phys. Rep. **442**, 109 (2007).
[8] J. Schaffner and I.N. Mishustin, Phys. Rev. C **53**, 1416 (1996).
[9] A. Burrows and J.M. Lattimer, Astrophys. J. **307**, 178 (1986).
[10] W. Keil and H.T. Janka, Astron. & Astrophys. **296**, 145 (1995).
[11] J.P. Blaizot, Phys. Rep. **64**, 171 (1980).
[12] M. Prakash and K.S. Bedell, Phys. Rev. **C** 31, 1118 (1985).
[13] B.A. Brown, Phys. Rev. Lett. **85**, 5296 (2000).
[14] K.A. Brueckner, S.A. Coon, J. Dabrowski, Phys. Rev. **168**, 1184 (1967).
[15] P.J. Siemens, Nucl. Phys. **A141**, 225 (1970).
[16] A. Akmal, V.R. Pandharipande and D.G. Ravenhall, Phys. Rev. C **58**, 1804 (1998).
[17] B.D. Serot and J.D. Walecka, Adv. Nucl. Phys. **16**, 1 (1986).
[18] R. Pak *et al.*, Phys. Rev. Lett. **78**, 1022 (1997).
[19] B.-A. Li, C.M. Ko, and Z.Z. Ren, Phys. Rev. Lett. **78**, 1644 (1997).
[20] L.W. Chen, C.M. Ko, and B.-A. Li, Phys. Rev. Lett. **94**, 032701 (2005); Phys. Rev. C **72**, 064309 (2005).
[21] D.V. Shetty, S.J. Yennello and G.A. Souliotis, Phys. Rev. C **76**, 024606 (2007).
[22] M. Centelles, X. Roca-Maza, X. Viñas, and M. Warda, Phys. Rev. Lett. **102**, 122502 (2009).
[23] B.K. Sharma and S. Pal, Phys. Lett. **B682**, 23 (2009).
[24] G.A. Lalazissis, J. König, and P. Ring, Phys. Rev. C **55**, 540 (1997).
[25] B.G. Todd and J. Piekarewicz, Phys. Rev. Lett. **95**, 122501 (2005).
[26] C.J. Horowitz and J. Piekarewicz, Phys. Rev. Lett. **86**, 5647 (2001); Phys. Rev. C **66**, 055803 (2002).
[27] H. Müller and B.D. Serot, Phys. Rev. C **52**, 2072 (1995).
[28] P. Wang, Phys. Rev. C **61**, 054904 (2000); P. Wang, D.B. Leinweber, A.W. Thomas and A.G. Williams, Nucl. Phys. **A748**, 226 (2005).
[29] B.K. Sharma and S. Pal, Phys. Rev. C **81**, 064304 (2010).
[30] J.A. Pons, S. Reddy, M. Prakash, J.M. Lattimer and J.A. Miralles, Astrophys. J. **513**, 780 (1999).
[31] C. Ishizuka, A. Ohnishi, and K. Sumiyoshi, Nucl. Phys. **A723**, 517 (2003).
[32] A.S. Botvina and I.N. Mishustin, Phys. Lett. **B584**, 233 (2004).
[33] G. Röpke, Phys. Rev. C **79**, 014002 (2009).
[34] S. Typel, G. Röpke, T. Klähn, D. Blaschke, and H.H. Wolter, Phys. Rev. C **81**, 015803 (2010).
[35] F.J. Fattoyev and J. Piekarewicz, Phys. Rev. C **82**, 025810 (2010).
[36] H. Pais, A. Santos, and C. Providência, Phys. Rev. C **80**, 045808 (2009).
[37] D.J. Millener, C.B. Dover, and A. Gal, Phys. Rev. C **38**, 2700 (1988).
[38] C.B. Dover and A. Gal, Ann. Phys. (N.Y.) **146**, 309 (1983).
[39] T. Fukuda *et. al.*, Phys. Rev. C **58**, 1306 (1998).
[40] P. Khaustov *et. al.*, Phys. Rev. C **61**, 054603 (2000).
[41] C.J. Batty, E. Friedman, and A. Gal, Prog. Theor. Phys. Suppl. **117**, 227 (1994).
[42] E. Friedman and A. Gal, Phys. Rep. **452**, 89 (2007).
[43] R.C. Tolman, Phys. Rev. **55**, 364 (1939); J.R. Oppenheimer and G.M. Volkoff, *ibid* **55**, 374 (1939).
[44] J.M. Weisberg and J.H. Taylor, Phys. Rev. Lett. **52**, 1348 (1984).
[45] G. Baym, C.J. Pethick, and P. Sutherland, Astrophys. J. **170**, 299 (1971).